Technologisch Instituut-K.VIV
Mechanical Separation and
Particle Technology

Volume 8

PROCEEDINGS Part III

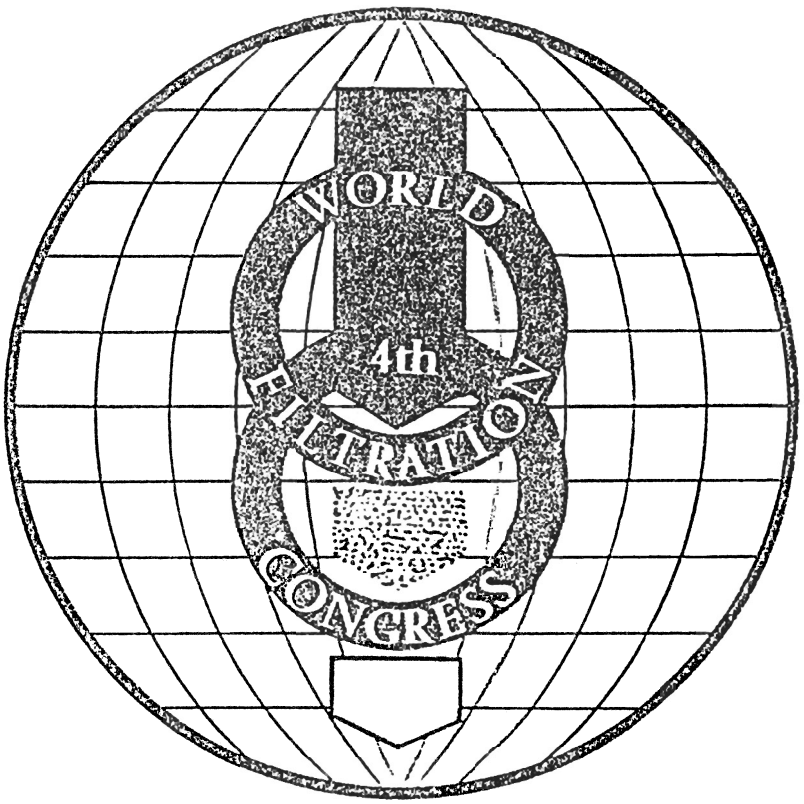

22 - 25 April 1986
Ostend, Belgium

Editors : R. Vanbrabant
J. Hermia
R.A. Weiler

The Royal Flemish Society of Engineers (K.V.I.V.) Antwerp (Belgium)
329th event of the European Federation of Chemical Engineers

DEWATERING OF FILTER CAKE BY VACUUM, PRESSURE AND PRESSURE/VACUUM FILTRATION

Dipl.-Ing. H. Anlauf , Prof. Dr.-Ing. W. Stahl
Institut für Mechanische Verfahrenstechnik und Mechanik
der Universität Karlsruhe (TH), D-7500 Karlsruhe 1

ABSTRACT

The aim of this study was to describe the dewatering kinetics of very fine filter cakes through which air is passed through.

The pertinent experiments were adapted as closely as possible to filtration conditions in practice.

Extensive laboratory filtration tests were performed with a great variety of concentrates from ore, mineral and coal beneficiation.

An analysis of the dewatering results gives a comparison of possible degree of saturation of filter cake and compressed air requirement.

This helped optimizing filtration. A purely mechanical dewatering of filter cake by pressure filtration proved to be an interesting alternative to the conventional combination of vacuum filtration and thermal drying.

INTRODUCTION

Generally, continuous vacuum filters are applied for dewatering fine-grain concentrates in beneficiation plants.

The tendency worldwide towards fine-grain products leads in many cases to unsatisfactory dewatering of the filter cake produced. As a result, vacuum filtration has often to be combined with thermal drying.

Purely mechanical dewatering by continuous pressure filtration is a promising alternative.

For the design of continuous pressure filters it is necessary that cake formation and cake dewatering be described.

So far, the possibilities to do so have been insufficient especially with regard to filter cake dewatering [1]. The present study will assist filling this need.

TEST OPERATIONS AND TEST PRODUCTS

The necessary experiments were to be adapted as closely as possible to industrial filtration conditions.This led to the laboratory pressure filter unit shown in Fig. 1 [2].The measuring cell of the unit is discontinuously supplied with suspension. The filtering area is A=20 cm^2. Filter cake of a thickness of h_K = 5-30 mm may form. The differential pressure may be increased to Δp = 4 bar.Monofil and multifil industrial fabrics were used as filter cloth. The feed was concentrate from the iron ore, non-ferrous, coal and mineral beneficiation. About 20 limonitic, hematitic and magnetitic iron oxides, sulfidic copper, zinc, lead and iron ores, flotation coal as well as fluorite and barite were used.

All such products were difficult to filter. The average particle size of the solids was generally well under 50 µm. The particle size range was very broad. The fine grain portion was generally considerable and extended into the colloidal range.

Fig. 2 shows a typical zinc sulfide ore magnified 300 times. The considerable difference in particle size, the irregular shape and the rough surface of the grains are clearly to be seen.

CAKE FORMATION

First, structure and permeability of the filter cake had to be determined in dependence on differential pressue Δp and cake thickness h_K. One result was that all filter cakes had a more or less good compressibility. This is shown in Fig. 3 giving as an example the cake porosity ε of various products tested.

The porosity of the filter cake decreases with increasing filtration pressure.

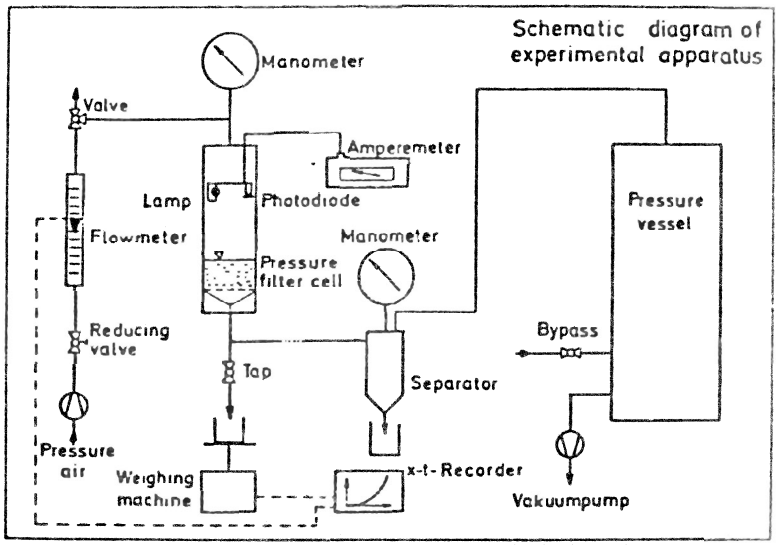

Fig. 1. Laboratory pressure filter

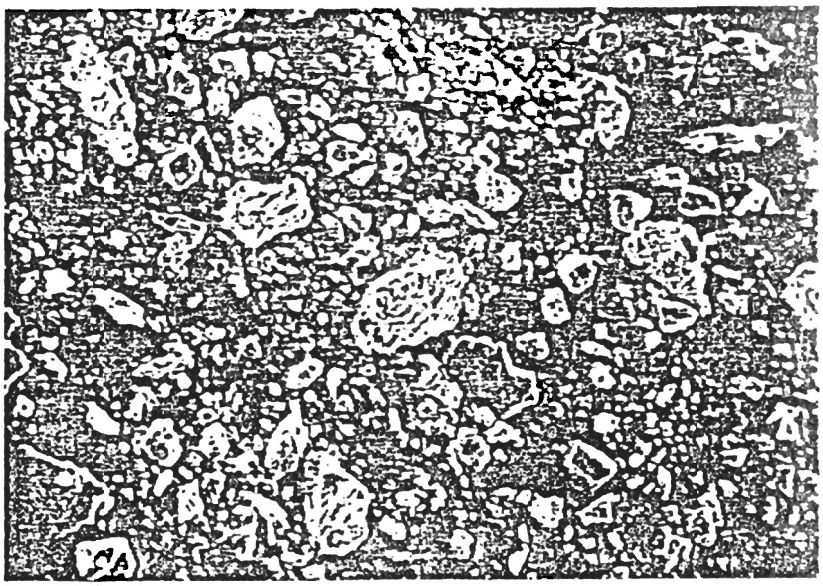

Fig. 2. ZnS-Ore particles

In agreement with the theory of compressible filter cake formation, a porosity gradient depending on the cake thickness could be observed [3].

With decreasing porosity the permeability P_C of the filter cake is decreased, too. Not only the filter cake but also the filter medium showed a flow resistance R_M which was pressure dependent.

Simplified, the cloth resistance may be described by an equivalent cake thickness h_{KE}. The absolute level of the differential pressure has no effect on the cake structure. In pure pressure and combined pressure/vacuum filtration corresponding porosity values resulted whereas the permeability differed sometimes to a larger extent.

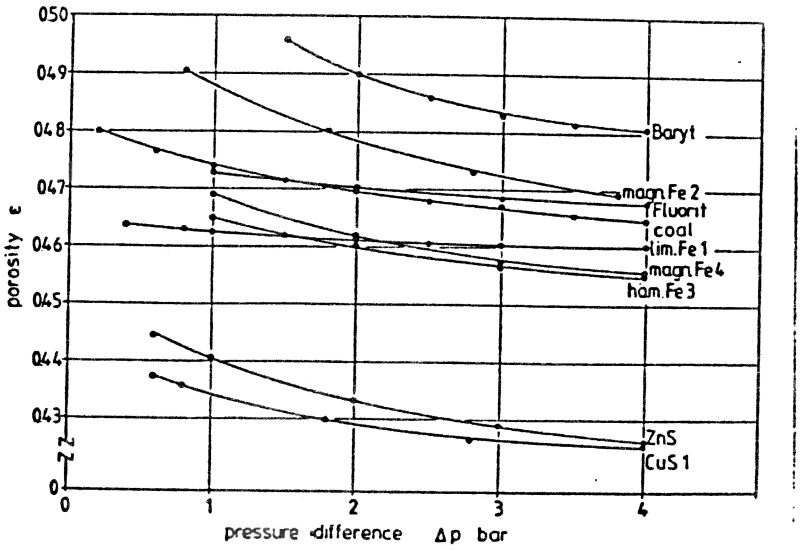

Fig. 3. Porosity of filter cakes

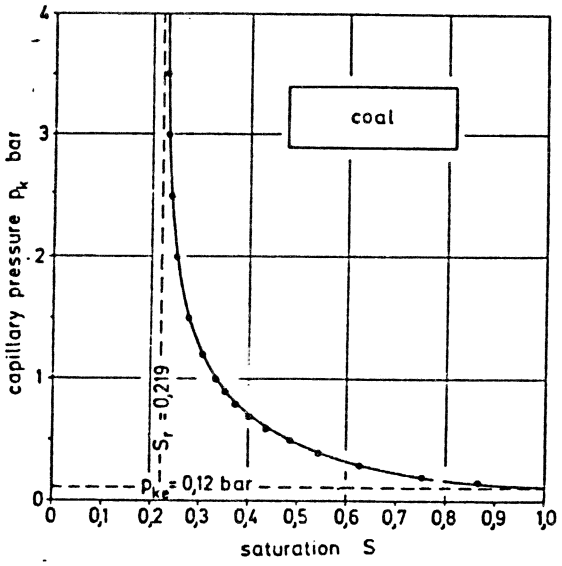

Fig. 4. Capillary pressure curve

The more the pressure level was decreased, i.e. the higher the vacuum portion of the total differential pressure was, the easier dissolved air was desorbed from the liquid. At an unfavourable ratio of capillary forces and pressure gradient, pore blockade was caused by gas bubbles.

Porosity, cake permeability and cloth resistance cannot be calculated from the data of the respective particle size range. They have to be determined by test as material-specific functions.

DECREASE OF THE DEGREE OF SATURATION IN THE FILTER CAKE

The same applies to the capillary pressure curve $p_K(S)$ for dewatering. In its product characterizing function it can also only be established by measurement. As the cake forming conditions have a considerable effect on the development of the pore structure, the capillary pressure curves for the products tested were determined directly from the filtration tests.

Fig. 4 gives an example of such a measured capillary pressure curve.

At complete pore saturation a minimum capillary inlet pressure p_{KE} has to be established first to achieve a first considerable dewatering of the cake. For low degrees of saturation the curve approaches the mechanical limit of dewatering S_r. Even when further increasing the pressure filtrate will not flow off any more.

After determination of the dewatering limits the dewatering kinetics may be examined.

In a separate test, dewatering up to the first air breakthrough $t_{2,0}$ through cake and filter cloth was examined. It was concluded from the result that, at the beginning of dewatering, displacement of the liquid from the filter cake does not proceed in a piston-like movement but individual large pores are emptied quickly so that, early, the liquid is relatively equally distributed throughout the material. This phenomenon is known from the literature under the termin "fingering" [4].

This early equalization of the liquid distribution throughout the filter cake enables that the complete phase of mechanical dewatering be determined together.

The capillary pressure curve is of fundamental importance for the dewatering of filter cake. Overcoming of the capillary forces by the pressure gradients in the gas phase is decisive for the liquid flow off. Frictional forces caused by the flowing gas can, in this respect, be neglected. Also, the influence of thermal dewatering by evaporation was negligible with the short dewatering times of about 180 s.

The choice of the pressure level did not play a significant role on the dewatering result. Comparable degrees of saturation were obtained in the sole pressure and pressure/vacuum filtration.

The basis for the description of dewatering was the Darcy equation. It has to be adapted to the conditions of the two-phase flow which led to a dewatering coefficient known from literatur [5]. Characterizing the capillary pressure effect in this coefficient by means of an average pressure appeared to be too simple.

Only after the complete capillary pressure distribution was included in the calculation measured results did agree satisfactorily with the calculation.

Dewatering of homogeneous filter cakes may be described by the following equation:

$$\frac{dS}{dt} = \frac{2 \cdot P_c(\Delta p) \cdot P_{c,rel,l}(S) \cdot (\Delta p - p_K(S))}{\varepsilon(\Delta p) \cdot \eta_l \cdot (h_K + h_{KE})^2} \qquad (1)$$

Decrease of saturation degree S with time t is described in dependence on chosen parameters such as differential pressure Δp and cake thickness h_K as well as in dependence on product characteristics such as specific permeability P_c, relative liquid permeability $P_{c,rel,l}(S)$, capillary pressure distribution $P_k(S)$, porosity, equivalent cake thickness h_{KE} and liquid viscosity.

Figures 5 and 6 show the result of the calculation according to equation 1 for a number of products tested. The measured saturation degree is always plotted above the calculated one. The chronological progress of each test is shown by a curve.

Generally, the deviations between calculation and measurement are less than S=0.05. Where larger deviations occurred the cake was found to be inhomogeneous. Finest suspended particles in the suspension concentrated in the upper slurry zone and deposited in the cake top layers. Where the cake is not or only insufficiently homogeneous the dewatering behaviour of a product may be determined by computational interpolation in dewatering diagrams.

Fig. 7 gives an example.

The dewatering progress has first to be measured for 16 different combinations of differential pressure and cake thickness. When plotting for these combinations the residual humidity for a constant dewatering time on the shown three dimensional diagram, spacial areas result. With these dewatering diagrams any operating point can be determined by computational interpolation.

Although this method does not give information on the material characteristics it is practically always applicable with a great accuracy.

GAS THROUGHPUT THROUGH PARTIALLY DEWATERED FILTER CAKE

After determination of the dewatering result in form of the achievable degree of saturation the amount of compressed air required for such dewatering was then to be determined.

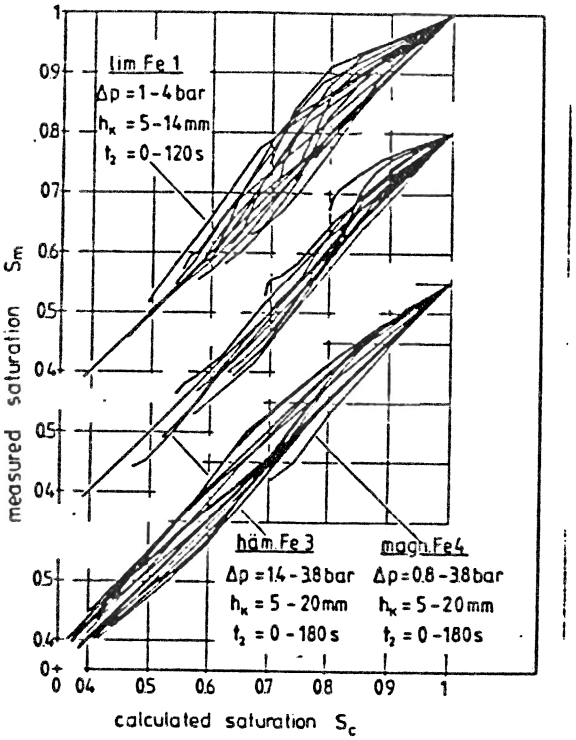

Fig. 5. Dewatering of iron ores

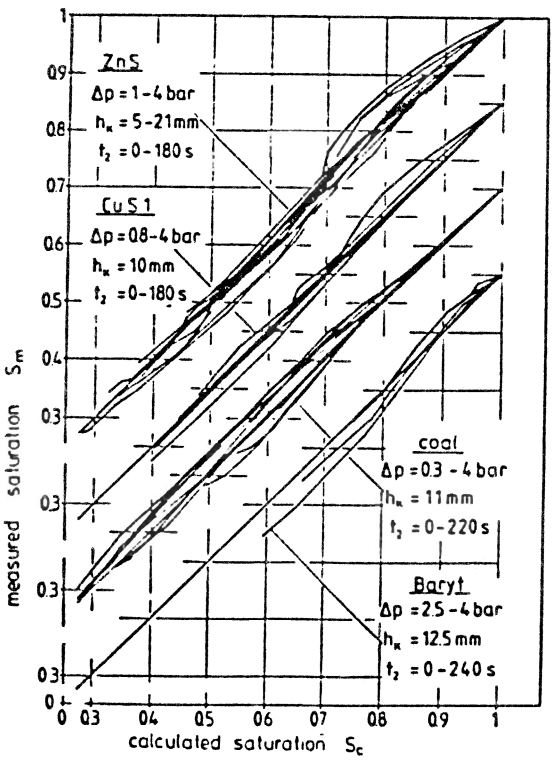

Fig. 6. Dewatering of non iron ores

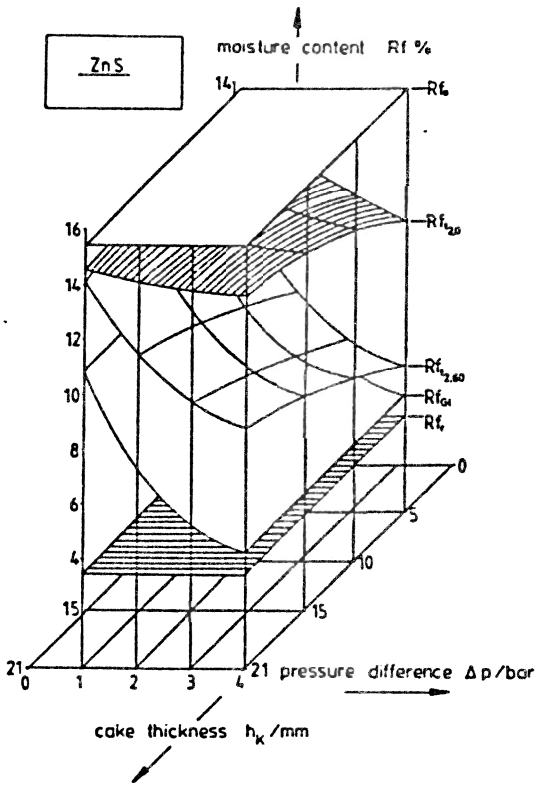

Fig.7. 3-dimensional dewatering diagram

The Darcy equation can also be used to describe the air throughput through partially dewatered filter cake. In this case air is used as compressible flow medium. The pore space constantly changing during dewatering may be described by means of the relative gas permeability $P_{c,rel,g}(S)$.

$$\dot{V}_{g,e} = \frac{P_c \cdot P_{c,rel,g}(S) \cdot p_m \cdot \Delta p \cdot A}{\eta_g \cdot P_o \cdot (h_K + h_{KE})} \qquad (2)$$

This equation for the volumetric gas flow at the cake inlet $\dot{V}_{g,e}$ was also known from literature in a similar form [6]. The compressibility of air is taken into account by the dependence of the gas condition on the ratio of the pressure P_o above the cake to the average pressure P_m^o.

The chronological development of the volumetric gas stream cannot yet be calculated from equation 2. It is necessary to have data on the decrease of saturation degree with time since the gas throughput is not caused but consequence of dewatering.

As may be seen in Fig. 8 the measuring

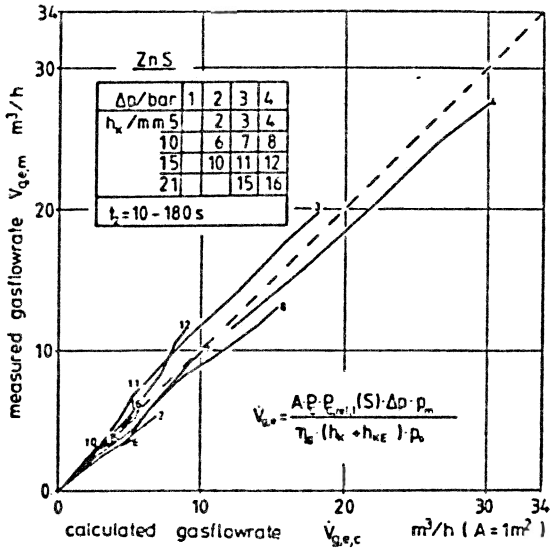

Fig. 8. Gas flow rates through filter cakes of ZnS-ore

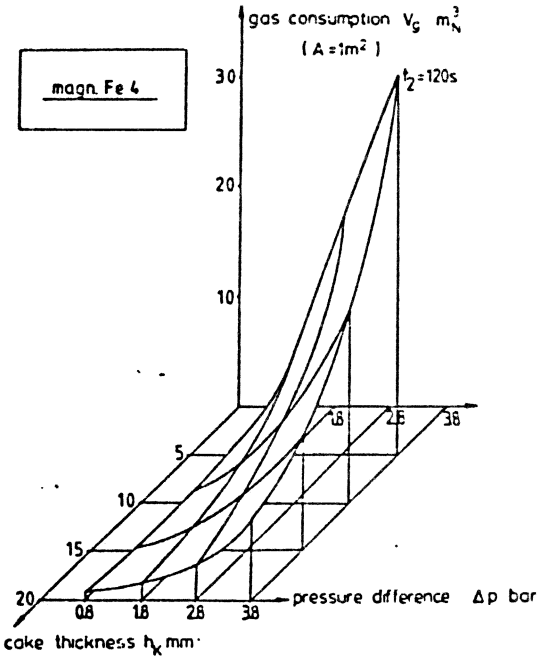

Fig. 9. 3-dimensional gas consumption diagram

results from this model equation are generally correct.

A prerequisite for this is again a homogeneous pore system. If this is not the case, interpolation may be applied in the gas consumption diagrams similar to the dewatering diagrams.

The gas consumption diagram of Fig. 9 shows the considerable increase in gas consumption at low cake thickness and high pressure.

COMPARISON OF EXPENDITURE AND RESULT OF DEWATERING

The energy requirement for compression of air to flow through the cake progresses with increasing degree of dewatering. For the dewatering times technically applied, the energy consumption for air compression is as a rule considerably less than for thermal drying. This is demonstrated in Fig. 10 for the dewatering of iron ore.

It shows a comparison of energy consumption for mechanical and thermal dewatering. The basis for this comparison is a residual humidity of 10% which can be reached by vacuum filtration. The curve for the specific mechanical energy w shows the energy required to further reduce the humidity by increasing the pressure. The other curve shows the thermal energy necessary to further dry the solids material.

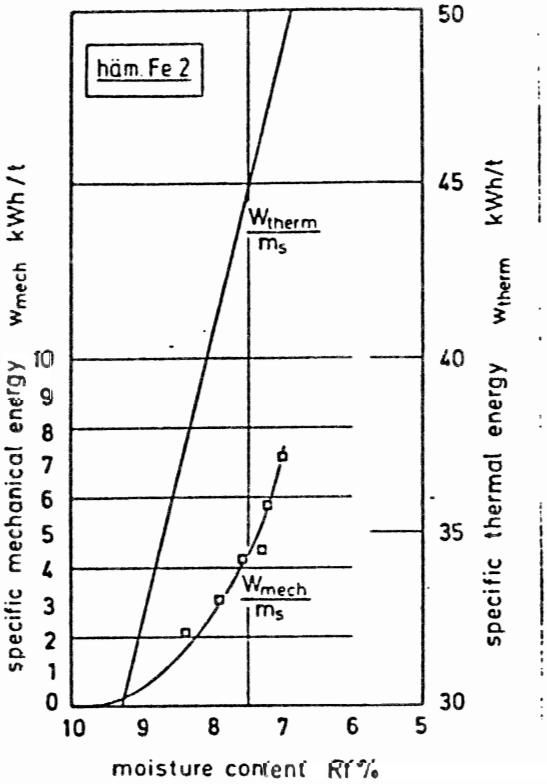

Fig. 10. Energy consumption for air compression and thermal drying

Even with very tough mechanical conditions (in this case ΔP = 3.8 bar) the energy requirement for thermal drying is 7 times larger than for gas compression.

This shows that as a rule the energy consumption for purely mechanical dewatering is by far more favourable than for mechanical/thermal dewatering. As shown in Fig. 11 there is no general tendency to optimize mechanical dewatering.

The specific gas compression energy w is plotted against the solids mass m per unit of time. All results lead to a degree of saturation of S = 0.60. The curves shown are based on a computer simulated dewatering operation. The material functions necessary to solve equations 1 and 2 originate from tests.

A general basis for the dewatering of the best operating method of a pressure filter cannot be given. It is necessary that in addition to the degree of saturation, which can be achieved, the solids quantity per time be known.

SUMMARY

On the basis of extensive filtration tests closely relating to practice, methods have been established to describe the dewatering procedure. The chronological progress for the degree of saturation and gas throughput may be analytically determined in dependence on various parameters.

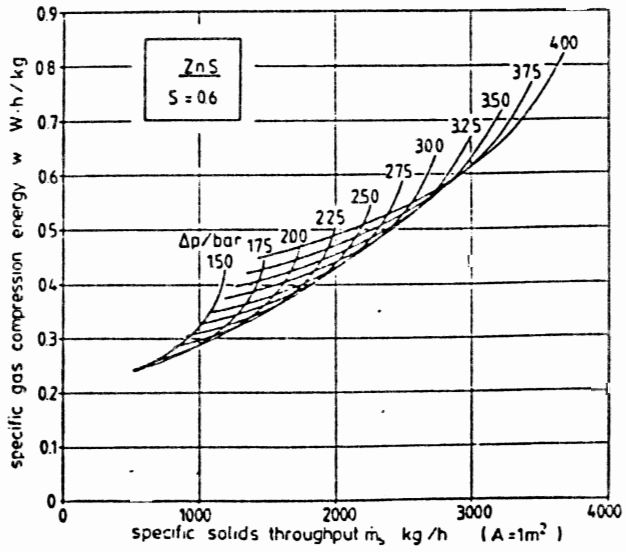

Fig. 11. Energy for gas compression under various dewatering conditons

This enables to optimize mechanical dewatering.

If a required degree of saturation can be achieved purely mechanically by pressure filtration this is far more favourable in respect of energy consumption than a combination of insufficient vacuum filtration followed by thermal drying.

References

[1] H. Schubert: Kapillarität in porösen Feststoffsystemen, Springer Verlag (1982), 264-265

[2] W. Stahl, H. Anlauf, R. Bott
Untersuchungen zur optimalen Flüssigkeitsabtrennung bei der Aufbereitung schwieriger Erze durch kontinuierliche Vakuum-Druck- und hyperbare Vakuumfiltration.
BMFT-FB-T84-232 (1984), 6-11

[3] F.M. Tiller
What the filter man should know about theory, Filtration & Separation (1975) 7/8, 386-394

[4] L. Paterson, V. Hornof, G. Neale
A consolidated porous medium for the visualization of unstable displacements, Powder Technology 33 (1982), 265-268

[5] → [1], 268

6 → [1], 269